Influence of Drag Reducing Polymers on Turbulent Mass Transfer to a Pipe Wall

GEORGE A. McCONAGHY
and
THOMAS J. HANRATTY
University of Illinois
Urbana, Illinois

Completely developed and entry region mass transfer rates in turbulent pipe flow of drag reducing polymer solutions were studied experimentally using electrochemical techniques. The percent change in the fully developed mass transfer rate at a given volumetric flow was found to be greater than the percent change in the pressure gradient. The data are interpreted by using the law of the wall, valid for Newtonian fluids at large Schmidt numbers, whereby K^+ is related to $Sc^{-0.74}$. The proportionality constant is correlated with percent drag reduction and is found to decrease with increasing drag reduction. The use of an analogy between momentum and mass transfer predicts a somewhat greater mass transfer reduction than was observed.

SCOPE

A number of investigators (Corman, 1970; Debrule, 1972; Gupta et al., 1967; Morrucci and Astarita, 1967; McNally, 1968; Smith et al., 1969) have established that drag reducing polymers can cause a reduction in the rate of turbulent heat transfer between a wall and aqueous solutions with Prandtl numbers in the range of 5 to 10. This paper describes a study of turbulent mass transfer in a pipeline with a diameter of 2.61 cm. Entry region and fully developed mass transfer coefficients are presented for dilute solutions of the high molecular weight polyacrylamide, Separan AP-30, at Reynolds numbers from 13 000 to 86 500.

These measurements were made using an improved electrochemical technique applicable to drag reducing aqueous solutions. The results are of particular interest since they give information on scalar transport at high Schmidt numbers, from 950 to 1 260. A form of the Reynolds analogy is examined to see if it can relate mass transfer to momentum transfer for drag reducing solutions.

CONCLUSIONS AND SIGNIFICANCE

The percent change in the fully developed mass transfer rate at a given volumetric flow is found to be greater than the percent change in pressure gradient. The decrease in the mass transfer rate caused by the addition of drag reducing polymers is associated with changes in both the turbulence close to the wall and the Schmidt number.

The law of the wall relation

$$\frac{K_\infty}{u^*} = BSc^{-0.74} \qquad (1)$$

developed by Shaw (1976) for Newtonian fluids has been used to take into account the influence of Schmidt number. The coefficient B is correlated with percent drag reduction in Figure 9. It is found that it decreases with increasing drag reduction, being about 20% lower than for a Newtonian fluid at 40% drag reduction. This is consistent with the finding that turbulent velocity fluctuations normalized with the friction velocity u^* are smaller for drag reducing fluids than for Newtonian fluids in the region occupied by the concentration boundary layer. However, since no theory exists which correctly relates turbulent mass transfer to the fluctuating velocity close to a wall, it is not possible to relate the change in B to observed changes in turbulence properties close to a wall.

The analogy between momentum transfer and mass transfer agrees with the observation that the mass transfer rate is decreased more than the pressure gradient but overpredicts the amount by which mass transfer rate is decreased.

RELATION TO PREVIOUS WORK

Mass transfer rates at high Schmidt numbers have been studied previously either by determining the decrease in weight of a soluble wall with time or by measuring the diffusion limited current flowing to a wall which is one of the electrodes of an electrolysis cell. Results obtained by the first of these methods are of uncertain reliability (Shaw, 1976) because as pointed out by Linton and Sherwood (1950) small fissures and surface roughnesses can develop while the dissolution is progressing. In previous work at this laboratory, Van Shaw (1963) and Son (1967) used the electrolysis method with Newtonian fluids to determine turbulent mass transfer rates to the wall of a circular tube by carrying out the ferricyanide-ferrocyanide redox reaction in the presence of a large excess of sodium hydroxide electrolyte. The only previous study of turbulent mass transfer in pipe flow of drag reducing solutions was carried out by Sidahmed and Griskey who used this electrolysis experiment to investigate mass transfer in dilute solutions of the polymer polyethylene oxide. These measurements were restricted to Reynolds numbers from 10 000 to 15 000 and to conditions of entry region mass transfer so that definite quantitative information about fully developed mass transfer rates could not be obtained. However, the results do indicate that the mass transfer rate is reduced in polymer solutions.

We initially attempted to use the ferricyanide-ferrocy-

Correspondence concerning this paper should be addressed to Thomas J. Hanratty, Department of Chemical Engineering, University of Illinois, Urbana, Illinois 61801.

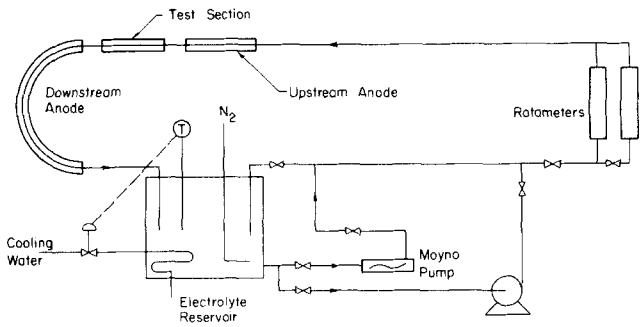

Fig. 1. Flow system.

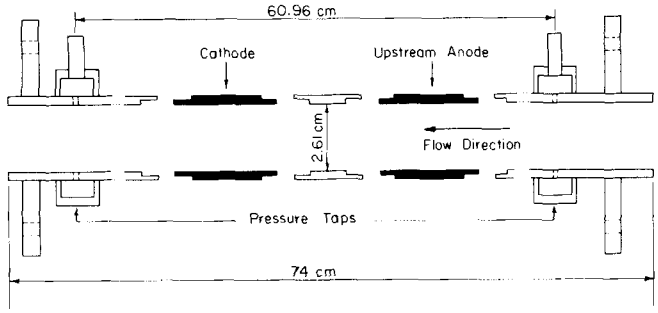

Fig. 2. Mass transfer test section.

anide electrolysis reaction to study the influence of dissolved polyethylene oxide and of dissolved Separan AP-30, a high molecular weight polyacrylamide, on fully developed mass transfer rates. We found that the drag reducing polymers degraded so rapidly in the presence of sodium hydroxide that meaningful measurements could not be made. Therefore, we sought an electrochemical system in which polymer degradation is minimal and selected the diffusion limited cathodic reduction of tri-iodide ion in a potassium iodide electrolyte. This system did not cause serious chemical degradation of drag reducing polymers.

DESCRIPTION OF EXPERIMENTS

We used this tri-iodide/iodide electrolysis system to investigate turbulent mass transfer to the wall of a 2.61 cm diam. circular tube for dilute solutions of the high molecular weight polyacrylamide Separan AP30, with concentrations ranging from 50 to 325 p.p.m. We measured both the entry region and fully developed mass transfer coefficients at Reynolds numbers ranging from 13 000 to 86 500. The majority of measurements were made under conditions where both the concentration and velocity fields were fully developed. Preliminary experiments to study entry region mass transfer were done mainly to characterize the influence of drag reducing polymers on the mass transfer entry length and to assure that subsequent measurements were made where the concentration boundary layer had become fully developed. The pressure drop and mass transfer coefficient were measured simultaneously with the same test section so that the reduction of the mass transfer rate and pressure gradient could be compared directly.

The experiments were carried out in the flow loop built by Van Shaw (1963) and shown in Figure 1. A 427 cm long section of straight pipe preceded the test section to insure that the flow field was fully developed. The electrolytic solution was circulated by a one-stage screw type of Moyno pump to minimize mechanical degradation of the shear-sensitive polymer. Figure 2 shows the 2.61 cm diam. test section in greater detail. This test section was designed to accommodate cathodes of both 6.35 and 8.26 cm length which were made of platinum plated brass tube having the same inside diameter as the adjoining Plexiglas segments of the test section. The anode consisted of a platinum plated brass section 6.35 cm in length upstream from the cathode and a 152 cm length of nickel pipe downstream from the cathode.

Piezometer ring pressure taps were located 60.96 cm apart. Each had four 1.6 mm diam. holes drilled through the tube wall at locations 90 deg. apart. An enclosed Plexiglas annulus, 2.54 cm wide and 0.64 cm deep, was glued around the holes. The pressure drop between the two pressure taps was measured with manometers using either Merian fluids D7878 (specific gravity = 1.200) or D8325 (specific gravity = 1.75).

The electrolyte used in the measurements consisted of iodine (3×10^{-4} to 10^{-3}M) dissolved in 0.5 M potassium iodide solution. This system has been studied by Newson and Riddiford (1961) and by Chin (1971). The reactions occurring at the cathode and anode were

$$\text{Test electrode (cathode)} \qquad I_3^- + 2e^- \rightarrow 3I^-$$

$$\text{Reference electrode (anode)} \qquad 3I^- \rightarrow I_3^- + 2e^-$$

The anodes were at ground potential, and the negative potential of the cathode was kept large enough that the cathodic reaction was diffusion limited. That is, the reaction rate was fast enough that the concentration of the tri-iodide ion at the cathode surface was close to zero. Under these circumstances, the mass transfer coefficient K is determined by measuring the electric current flowing in the electrolysis cell I:

$$K = \frac{I}{n_e F A C_B} \tag{1a}$$

The electrical circuitry used to control the voltage and to measure I has been described in a number of previous papers from this laboratory (Fortuna and Hanratty, 1972; Son, 1967), and in a thesis by McConaghy (1974).

The cathode shown in Figure 3*a* was used to determine the distance from the upstream edge at which the concentration boundary layer became fully developed. The cathode body was an 8.26 cm long brass tube. Platinum wires with diameters of 1.02 mm were secured in holes 1.27, 1.90, 2.54, 3.17, 3.81, 5.05, and 6.35 cm from the upstream edge with Cycleweld epoxy glue which also insulated them from the surrounding metal surfaces.

The measurements of the mass transfer coefficient under fully developed conditions were obtained with the cathode shown in Figure 3*b*. The cathode body was a 6.35 cm long brass tube. The local mass transfer coefficient was determined at a position 5.05 cm from the upstream edge of the cathode by measuring the current flowing to one of the test electrodes embedded in the cathode. At this position, a 1.59 mm deep by 6.35 mm long by 38.1 mm wide slot was milled in the outside wall of the tube. At midlength in the slot, ten small holes were drilled through the wall to admit five 0.320 mm and five 0.643 mm diam. circular platinum wires. The holes were 2.29 mm apart and were 0.25 mm larger in diameter than the corresponding platinum wires. The wires were glued in place as just described.

The finishing procedure for the two cathodes shown in Figure 3 was the same. The inside wall of the brass tube was polished with Sandwet 200 silicon carbide paper to remove roughness resulting from machining. Then the circular test electrodes were glued as described above. After the glue had set for 48 hr, the inside surface was polished successively with Sandwet 400 nnd 600 silicon carbide paper to remove excess epoxy cement and give the surface a very smooth finish. Finally, the surface was treated with

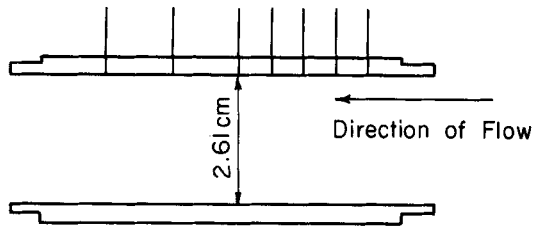

a) Cathode to Study Mass Transfer Entry Region

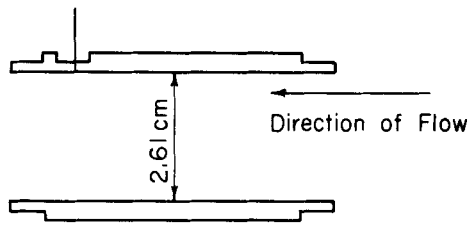

b) Cathode to Study Fully Developed Mass Transfer

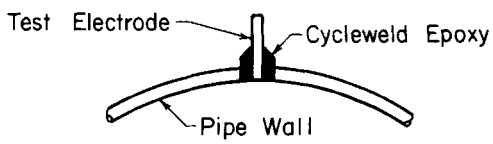

c) Test Electrode Details

Fig. 3. Cathode elements.

polishing compound and rinsed thoroughly with warm soap solution in preparation for plating. The test sections were plated with Engelhard platinum plating solution No. 209 at 93°C for 45 min. Details of the plating procedure are given by Shaw (1976). The entire inside wall of the cathode is then a smooth platinum surface with a number of isolated circular elements to measure local mass transfer rates.

The electrolyte and polymer solutions were prepared fresh before each experiment by following a standard procedure. Potassium iodide and iodine were added to deionized water, and the solution was mixed with an electric stirrer until dissolution was completed. Six liters of a concentrated 0.5 wt % aqueous solution of Separan AP-30 were prepared separately. This was done by sprinkling the polymer powder slowly onto the surface while the solution was mixed gently. This polymer master solution was mixed for at least 4 hr to insure that it was clear and free from gelled lumps of undissolved polymer. At the same time, the electrolyte was pumped through the flow loop until stable conditions of temperature and flow rate were attained. The required amount of master polymer solution was then added to the electrolyte to obtain the desired concentration. Mass transfer measurements commenced when the flow rate and pressure drop attained steady values.

The concentration of iodine was determined by titration with sodium thiosulfate using starch as an indicator. The kinematic viscosity of all solutions were measured with a Cannon-Fenske capillary viscometer. Diffusion coefficients of tri-iodide, measured in the Couette flow apparatus described by Fortuna (1972), are summarized in Table 1. The measurement for the electrolyte is very close to the value of 1.13×10^{-5} reported by Newson and Riddiford (1961) for 0.1 M *KI*. The diffusion coefficient measured

TABLE 1. DIFFUSION COEFFICIENT FOR TRI-IODIDE IONS

Separan AP-30 concentration, p.p.m.	D, cm²/s
0	1.15×10^{-5}
25	0.95
50	0.92
100	0.86
200	0.92
400	0.88

in the polymer solutions is lower than in the electrolyte solvent but did not decrease systematically with increasing polymer concentration in the range of these experiments. An average of the values shown in Table 1 for the polymer solutions was used to calculate the Schmidt number characterizing the mass transfer measurements with drag reducing solutions.

RESULTS

Friction Factors

The pressure drop was measured simultaneously with the mass transfer rate during all experiments. Fanning friction factors

$$f = \frac{d}{4}\left(\frac{\Delta P}{L}\right) \Big/ \frac{1}{2}\rho U_B^2 \qquad (2)$$

calculated from these measurements are shown in Figure 4. The range of Reynolds numbers was 13 100 to 86 500 for the solvent and 17 950 to 54 900 for the polymer solutions, where the solution viscosity was used to compute the Reynolds number for the drag reducing fluids. The friction factor measurements for the Newtonian solvent agree well with the Blasius formula

$$f = 0.0791\, Re^{-1/4} \qquad (3)$$

The four solutions of Separan AP-30, having concentrations ranging from 50 to 325 p.p.m., show typical drag reducing behavior.

We used the definition of percent drag reduction adopted by a number of previous investigators (Hoyt, 1972; Lumley, 1969; Reischman, 1973):

$$\%\ \text{D.R.} = \left(1 - \frac{\Delta P_p}{\Delta P_s}\right)_Q \text{X100} \qquad (4)$$

The subscript Q indicates that the polymer solution is compared to the solvent at the same flow rate. The greatest drag reduction achieved in any of our experiments was about 55%.

Mass Transfer Entry Length

Mass transfer experiments were initially performed with the cathode shown in Figure 3*a* to determine the conditions for which the mass transfer process is fully developed. Measurements of the dimensionless local mass transfer coefficient $K^+ = K/u^*$ for the solvent are plotted in Figure 5 as a function of the dimensionless distance from the upstream edge of the cathode, $x^+ = \frac{xu^*}{\nu}$. These measurements indicate that the mass transfer coefficient is independent of x^+ for $x^+ > 1\,000$. The data show some scatter because of slight variations of the surface areas of the circular test electrodes.

Similar measurements were made for the 60 and 125 p.p.m. solutions of Separan AP-30. It was observed that the local dimensionless mass transfer coefficient is inde-

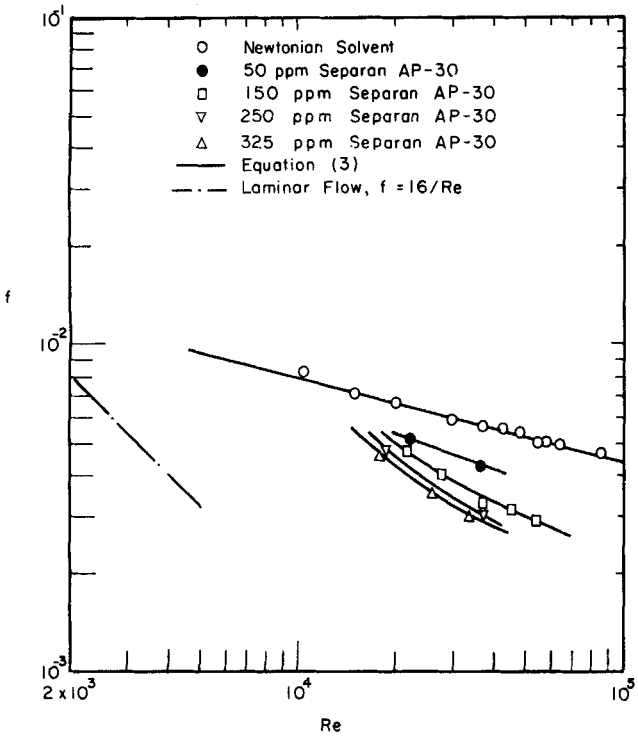

Fig. 4. Friction factor for solvent and polymer solutions.

pendent of x^+ over most of the cathode surface. The value of the mass transfer coefficient depended on the Reynolds number, amount of drag reduction, and Schmidt number of the solutions. It was found that these effects could be taken into account by normalizing the mass transfer coefficient by its limiting value, determined by the test electrode farthest downstream. The dependence of the normalized mass transfer coefficient K/K_∞ on axial distance x^+ is shown in Figure 6. The mass transfer coefficient for the polymer solution attains a fully developed value for $x^+ > 1\,000$. Eight of the points which fall significantly above the other data in Figures 5 and 6 are from the same electrode, which apparently had a deformed surface.

Local Fully Developed Mass Transfer Coefficients

The local mass transfer coefficients for a fully developed mass transfer boundary layer, determined using the cathode shown in Figure 3*b*, were made under conditions that the test electrode was at $x^+ \geq 1\,500$.

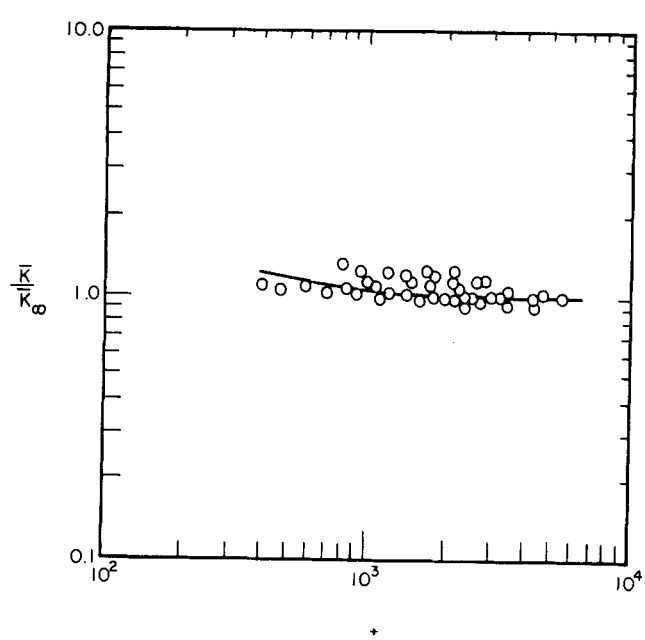

Fig. 6. Mass transfer entry length for polymer solutions.

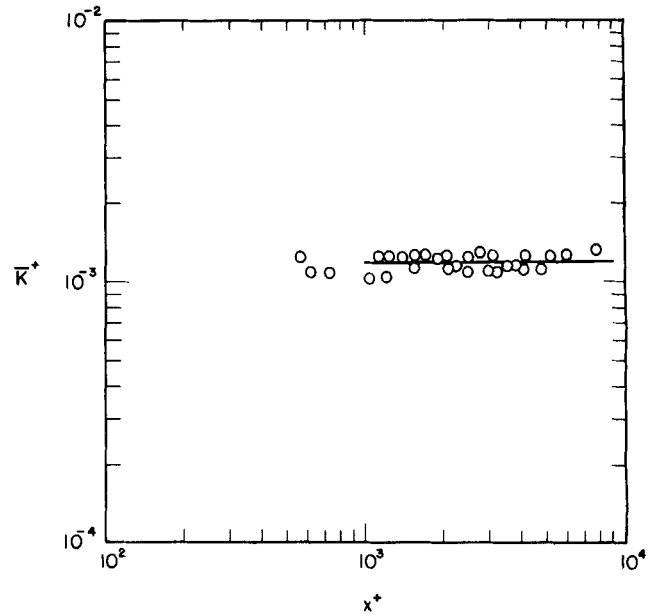

Fig. 5. Mass transfer entry length for solvent.

Values of $\overline{K}_\infty$ for the runs summarized in Figure 4 are presented in Table 2 and plotted in Figure 7. The mass transfer coefficient is clearly reduced by the addition of drag reducing polymers. A comparison of Figures 4 and 7 shows that the amount of mass transfer reduction is related to the amount of drag reduction. This is shown in Figure 8, where the percent mass transfer reduction defined as

$$\% \text{ MTR} = \left(1 - \frac{K_p}{K_s}\right)_Q \times 100 \qquad (5)$$

is plotted against the % DR. It is noted that the % MTR is greater than the % DR when the comparison is made at the same volumetric flow rate. There is no available theoretical explanation for the mass transfer coefficient being reduced more than the pressure gradient. An analogy based on eddy transport coefficients for drag reducing solutions, developed later in this paper, predicts mass transfer reduction illustrated by the dashed line in Figure 8. The analogy predicts an even greater reduction in mass transfer than was actually measured.

COMPARISON OF MASS TRANSFER MEASUREMENTS USING THE LAW OF THE WALL

The change in the mass transfer coefficient by the addition of drag reducing polymers is associated with changes of the Schmidt number as well as the turbulence properties. In order to take account of the influence of Schmidt number, we use law of the wall considerations.

For large Schmidt numbers, the concentration changes to its bulk value within the viscous sublayer. Consequently, the flow field within the concentration boundary layer is independent of the dimensions of the pipe and can be correlated using the friction velocity u^* as a characteristic velocity and the ratio of the kinematic viscosity and the friction velocity as a characteristic length ν/u^*.

Mass transfer data for large Schmidt numbers have also been correlated using this law of the wall. A dimensionless mass transfer coefficient is defined as $K_\infty^+ = K_\infty/u^*$. From dimensional considerations, it follows that

$$K_\infty^+ = f(Sc) \qquad (6)$$

Table 2. Average Mass Transfer Measurements in Solvent and Polymer Solutions

Re	U_b, cm/s	u^*, cm/s	Separan AP-30 concentration, p.p.m.	% D.R.	Sc	$\overline{K}_\infty^+$
13 120	39.9	2.42	—	—	692	1.04×10^{-3}
15 560	48.5	2.89	—	—	704	1.03
20 860	63.4	3.64	—	—	692	1.04
21 850	67.6	3.86	—	—	705	1.10
30 770	95.4	5.21	—	—	704	1.04
43 620	135.2	7.07	—	—	704	0.99
58 380	181.0	9.13	—	—	704	0.99
63 818	194.4	9.70	—	—	694	1.08
64 894	197.7	9.84	—	—	694	1.05
86 540	264.2	12.69	—	—	696	1.03
22 310	72.9	3.69	50	19	946	0.90
37 500	122.5	5.66	50	24	946	0.76
21 900	79.3	3.79	150	27	1 049	0.72
19 000	77.2	3.79	250	23	1 178	0.69
37 700	153.4	5.82	250	46	1 178	0.56
17 950	78.3	3.79	325	25	1 264	0.65
26 190	114.3	4.78	325	38	1 264	0.60
33 950	148.2	5.83	325	42	1 264	0.54
21 900	79.4	3.89	150	23	1 050	0.84
28 030	101.6	4.57	150	31	1 050	0.73
38 540	139.7	5.66	150	39	1 050	0.68
45 840	166.2	6.61	150	39	1 050	0.64
54 900	199.0	7.61	150	41	1 050	0.60
46 450	192.4	7.11	250	45	1 199	0.60

Shaw (1976) has recently determined empirically that the dependency on Schmidt number is given as

$$K_\infty^+ = B\, Sc^{-0.704} \tag{7}$$

We use this relation to compare mass transfer rates in polymer solutions with mass transfer rates in Newtonian fluids in Figure 9. Here

$$\frac{B_P}{B_N} = \frac{(K_x^+\, Sc^{-0.704})_P}{(K_x^+\, Sc^{-0.704})_N} \tag{8}$$

is plotted against the percent drag reduction. It is noted that B_P is less than that determined for a Newtonian solution. This indicates that the decrease in K_x for polymer solutions is greater than the decrease in friction velocity. These results are consistent with measurements of the influence of drag reducing polymers on velocity fluctuations close to the wall. These show that the root-mean-square value of the three components of the turbulent velocity fluctuations decrease more than would be indicated by the law of the wall.

Fortuna's (1972) measurements of the fluctuating velocity gradient at the wall indicate that close to a wall the

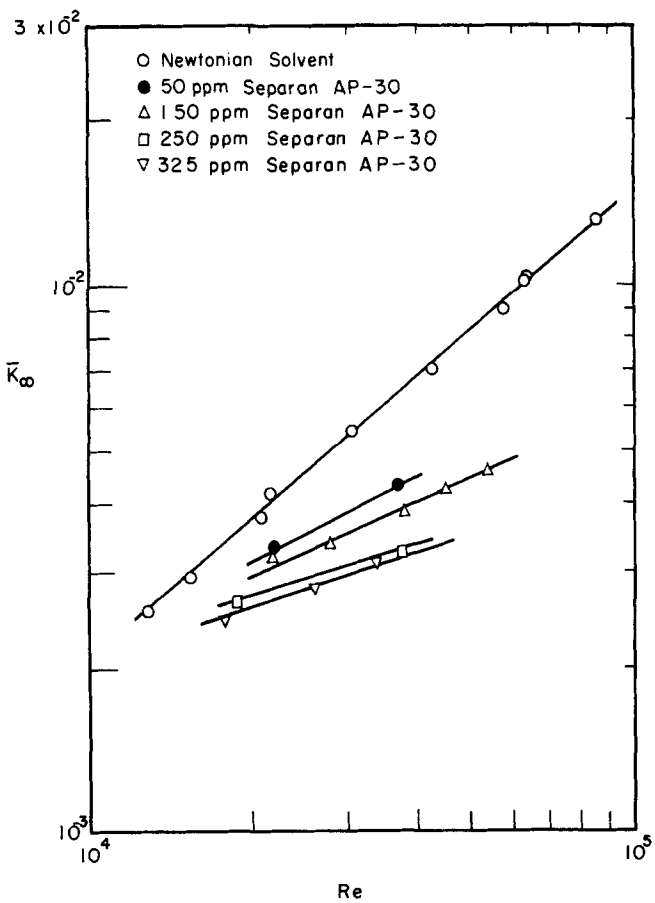

Fig. 7. Mass transfer coefficient in solvent and polymer solutions.

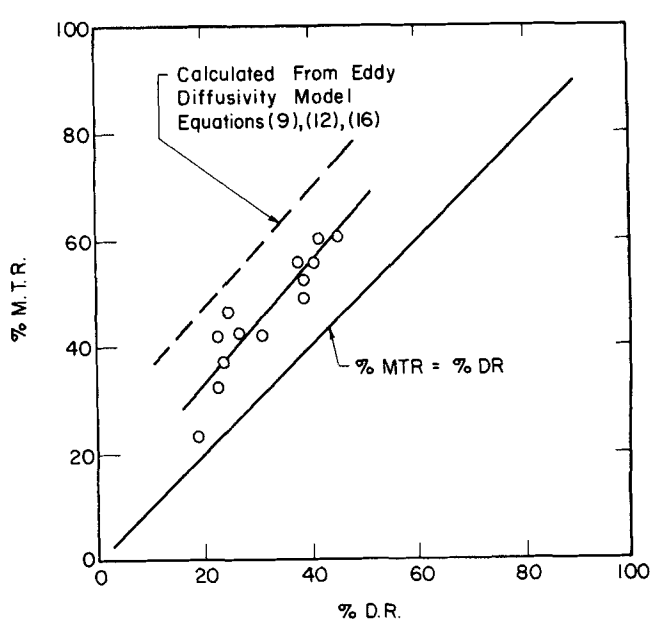

Fig. 8. Mass transfer reduction in polymer solutions.

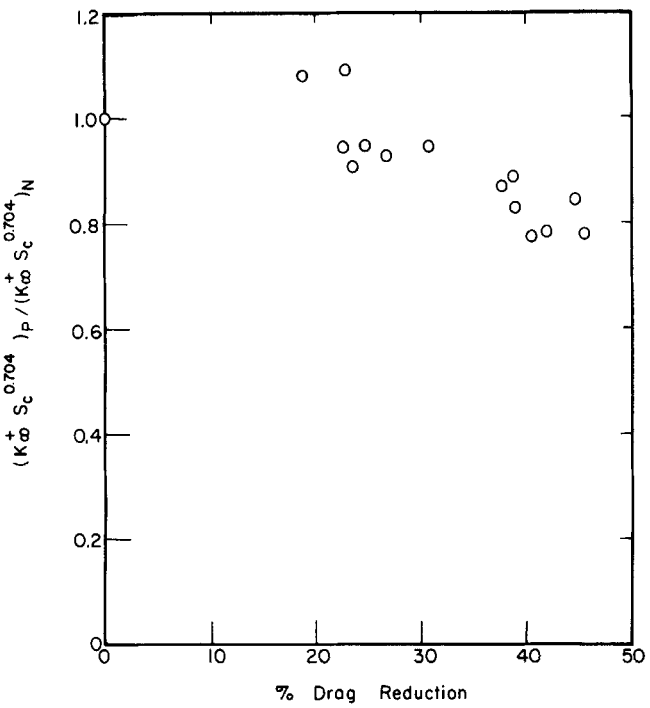

Fig. 9. Comparison of mass transfer coefficients for polymer solutions with mass transfer coefficients for Newtonian solutions using the law of the wall.

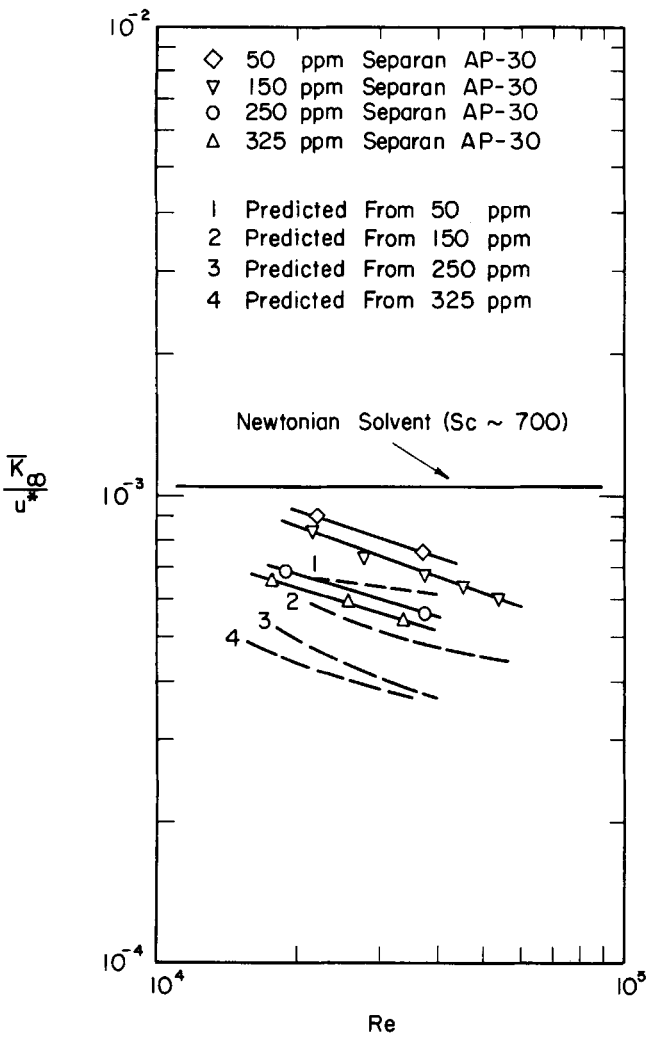

Fig. 10. Comparison of mass transfer coefficient predicted with Cess model to experimental measurements.

ratio of the root-mean-square values of the streamwise and transverse components of the fluctuating velocity to the local average velocity decreases with increasing drag reduction. Of more interest with respect to the interpretation of mass transfer data is the component of the turbulent velocity fluctuation normal to the wall. The measurements of Logan (1972) and of Carpenter (1973) show that the root-mean-square value of this component normalized with respect to the friction velocity is less in polymer solutions if the comparison is made at the same value of $y^+ = yu^*/\nu$.

At present no theory is available to relate turbulent mass transfer to the fluctuating velocity field close to a wall. Consequently, it is not possible to relate the reduction in the coefficient B in (7) to observed changes in turbulence properties close to a wall caused by the addition of drag reducing polymers.

INTERPRETATION OF MASS TRANSFER DATA USING AN ANALOGY WITH MOMENTUM TRANSFER

A number of previous investigations (Corman, 1970; Marrucci and Astarita, 1967; McNally, 1968; Poreh and Paz, 1969; Smith et al., 1969) have used an analogy to momentum transfer as a basis for interpreting results on the effect of drag reducing polymers on heat transfer. These analogies can be developed in terms eddy transport coefficients for momentum ϵ and for mass ϵ_M:

$$\tau = -(\nu + \epsilon)\frac{d\rho\overline{u}}{dy} \tag{9}$$

and

$$j = -(D + \epsilon_M)\frac{d\overline{c}}{dy} \tag{10}$$

where τ and j are the local momentum and mass fluxes in the y direction. The variation of ϵ with y is determined from velocity measurements, and ϵ_M is calculated by assuming it is related to ϵ. A relation between the mass transport coefficient and the friction factor is then determined by solving the mass balance equation. The usual assumption is that ϵ_M is directly proportional to ϵ:

$$\frac{\epsilon}{\epsilon_M} = Sc_t = \text{constant} \tag{11}$$

We have used the analogy in the form of (11) by assuming that the constant of proportionality is the same for drag reducing and Newtonian fluids. Because of the thinness of the concentration boundary layer at large Schmidt numbers, it is necessary to know the variation of ϵ within the viscous sublayer in order to apply the analogy. This presents difficulties, since measurements of $\overline{U}(y)$ in the viscous sublayer are insensitive to the choice of $\epsilon(y)$. Therefore, two empirical relations for $\epsilon(y)$ have been used for this purpose.

The eddy viscosity function suggested by Cess (1958)

$$\frac{\epsilon}{\nu} = \frac{1}{2}\left\{1 + \frac{\kappa^2 R^{+2}}{9}\left[1 - \left(\frac{r^+}{R^+}\right)^2\right]^2 \left[1 + 2\left(\frac{r^+}{R^+}\right)^2\right]^2 [1 - e^{-y^+/A_c^+}]^2\right\}^{1/2} - \frac{1}{2} \tag{12}$$

predicts the following relations for the viscous sublayer:

$$\frac{\epsilon}{\nu} = \frac{\kappa^2}{A_C{}^{+2}}(y^+)^4 \tag{13}$$

An expression devised by Leviton (1968)

$$\frac{\epsilon}{\nu} = \frac{\kappa R^+}{6}\left[1 - \left(\frac{r^+}{R^+}\right)^2\right]\left[1 + 2\left(\frac{r^+}{R^+}\right)^2\right]$$

$$[1 - e^{-(y^+/A_L^+)^2}] \quad (14)$$

has the following limiting form for small y^+:

$$\frac{\epsilon}{\nu} = \frac{\kappa}{A_L{}^{+2}} (y^+)^3 \quad (15)$$

Both the Cess and Leviton equations have two adjustable constants which are evaluated by comparing computed mean velocity profiles with experimental measurements. The von Karman constant in both equations κ has a value of 0.40 both for Newtonian and for drag reducing fluids (6). The one remaining adjustable constant A^+ accounts for viscous damping of turbulence near the wall. Values of $A_C{}^+ = 24.5$ and $A_L{}^+ = 23.0$ give the best agreement between calculated velocity profiles and Laufer's (1954) measurements.

Increasing values of A^+ correspond to an increasing thickness of the viscous wall region. Reischman (1973) has shown that the Cess eddy viscosity with $A_C{}^+$ larger than the Newtonian value describes his velocity profiles measured for polymer solutions. Values of $A_C{}^+$ and $A_L{}^+$ in Equations (13) and (14) can therefore be calculated by comparing measurements of the friction factor with solutions of the momentum balance equations using Equations (12) and (14).

As shown by Son (1967), a solution of the mass balance equation using Equations (11), (13), and (15) yields

$$K_\infty{}^+ = 0.900\ (Sc_t)^{-1/4} \left(\frac{0.40}{A_C{}^+}\right)^{1/2} Sc^{-3/4} \quad (16)$$

for the Cess relation and

$$K_\infty{}^+ = 0.827\ (Sc_t)^{-1/3} \left(\frac{0.40}{A_L{}^{+2}}\right)^{1/3} Sc^{-2/3} \quad (17)$$

for the Leviton relation. Different values of Sc_t are determined from (16) and (17) by comparing the calculated $K_\infty{}^+$ with measurements for Newtonian fluids.

Details of these calculations can be found in the thesis by McConaghy (1974), where calculated values of $K_\infty{}^+$ are compared with measurements reported in this paper. Results obtained with the Cess relation are shown in Figures 8 and 10. These are not much different from those derived from the Leviton equations.

The analogy is consistent with measurements in that it predicts a greater decrease of mass transfer rates than of pressure drop. However, as shown in both Figures 9 and 10, the analogy predicts a greater decrease in $K_\infty{}^+$ than what is measured. This suggests that the decrease in the magnitude of the turbulent velocity fluctuations caused by the addition of drag reducing polymers has a greater effect on momentum transfer than on mass transfer. This conclusion, however, should be accepted with reservation since, as suggested in a recent study by Shaw (1976), the analogy could be incorrect at large Schmidt numbers in that the equation describing the variation of ϵ_M has a different form than that for ϵ.

ACKNOWLEDGMENT

This work was partially supported by the National Science Foundation under Grants GK-2013 and GK-40745.

NOTATION

A = surface area of cathode, cm^2
$A_C{}^+$ = constant appearing in the Cess equation
$A_L{}^+$ = constant appearing in the Leviton equation
B = proportionality constant in Equation (7)
$\overline{C}$ = time averaged concentration, mole/cm^3
C_B = bulk averaged concentration, mole/cm^3
d = diameter of the tube, cm
D = molecular diffusion coefficient, cm^2/s
f = Fanning friction factor
F = Faraday's constant, 96 500 coul/equiv
I = current, amp
j = mass flux, mole/cm^2/s
K = mass transfer coefficient, cm/s
K^+ = dimensionless mass transfer coefficient, K/u^*
K_∞ = fully developed mass transfer coefficient
L = distance between pressure taps, cm
n_e = number of electrons in the reduction reaction
ΔP = pressure difference, g/cm^2 s
Re = Reynolds number = $d\ U_B/\nu$
R^+ = dimensional radius of the tube = Ru^*/ν
r^+ = dimensional radial distance = ru^*/ν
Sc = Schmidt number = ν/D
Sc_t = turbulent Schmidt number = ϵ/ϵ_M
$\overline{U}$ = time averaged streamwise velocity, cm/s
U_B = bulk averaged velocity, cm/s
u^* = friction velocity = $(\tau_w/\rho)^{1/2}$, cm/s
x^+ = dimensionless axial distance = xu^*/ν
y = distance from the wall, cm
y^+ = dimensionless distance from the wall = yu^*/ν

Greek Letters

ϵ = eddy viscosity, cm^2/s
ϵ_M = eddy diffusion coefficient, cm^2/s
κ = Von Karman constant
ν = kinematic viscosity, cm^2/s
ρ = density, g/cm^3
τ = shear stress or momentum flux, g/cm s^2
τ_w = shear stress at the wall, g/cm s^2

Subscripts

N = Newtonian fluid
P = polymer solution
S = electrolytic solution without polymer

LITERATURE CITED

Carpenter, C. N., "Drag Reduction Visual Study," Ph.D. thesis, Ohio State Univ., Columbus (1973).

Cess, R. D., "A Survey of the Literature on Heat Transfer in Turbulent Tube Flow," *Westinghouse Research Laboratories Rept. 8-0529-R24* (1958).

Chin, D. T., "An Experimental Study of Mass Transfer on a Rotating Spherical Electrode," *J. Electrochem. Soc.*, **118**, 1764 (1971).

Corman, J. S., "Experimental Study of Heat Transfer to Viscoelastic Fluids," *Ind. Eng. Chem. Process Design Develop.*, **9**, 254 (1970).

Debrule, P. M., "Friction and Heat Transfer Coefficients in Smooth and Rough Pipes with Dilute Polymer Solutions," Ph.D. thesis, Calif. Inst. Technol., Pasadena (1972).

Ernst, W. D., "Investigation of the Turbulent Shear Flow of Dilute Aqueous CMC Solutions," *AIChE J.*, **12**, 581 (1966).

Fortuna, G., and T. J. Hanratty, "The Influence of Drag-Reducing Polymers on Turbulence in the Viscous Sublayer," *J. Fluid Mech.*, **53**, 575 (1972).

Gupta, M. K., A. B. Metzner, and J. P. Hartnett, "Turbulent Heat Transfer Characteristics of Viscoelastic Fluids," *Intern J. Heat Mass Transfer*, **10**, 1211 (1967).

Hoyt, J. W., "The Effect of Additives on Fluid Friction," *Trans. A.S.M.E., J. Basic Eng.*, **94**, 252 (1972).

Laufer, J., "The Structure of Turbulence in Fully Developed Pipe Flow," *NACA Technical Rept. 1174* (1954).

Leviton, A. E., "A Correlation of Turbulent Temperature Profiles Using the Eddy Diffusivity Concept," M. S. thesis, Univ. Ill., Urbana (1968).

Linton, W. H., and T. K. Sherwood, "Mass Transfer from Solid Shapes to Water in Streamline and Turbulent Flows," *Chem. Eng. Progr.*, **46**, 258 (1950).

Logan, S. E., "Laser Velocimeter Measurement of Reynolds Stress and Turbulence in Dilute Polymer Solutions," Ph.D. thesis, Calif. Inst. Technol., Pasadena (1972).

Lumley, J. L., "Drag Reduction by Additives," *Ann. Rev. Fluid Mech.*, 1, 369 (1969).
Marrucci, G., and G. Astarita, "Turbulent Heat Transfer in Viscoelastic Liquids," *Ind. Eng. Chem. Fundamentals*, 6, 470 (1967).
McConaghy, G. A., "The Effect of Drag Reducing Polymers on Turbulent Mass Transfer," Ph.D. thesis, Univ. Ill., Urbana (1974).
McNally, W. A., "Heat and Momentum Transport in Dilute Polyethylene Oxide Solutions," *Naval Underwater Weapons Research and Engineering Station TR No. 44* (1968).
Meyer, W. A., "A Correlation of the Frictional Characteristics for Turbulent Flow of Dilute Viscoelastic Non-Newtonian Fluids in Pipes," *AIChE J.*, 12, 522 (1966).
Newson, J. D., and A. C. Riddiford, "Limiting Currents for the Reduction of the Tri-iodide Ion at a Rotating Platinum Disk Cathode," *J. Electrochem. Soc.*, 103, 695 (1961)
Poreh, M., and V. Paz, "Turbulent Heat Transfer to Dilute Polymer Solutions," *Intern. J. Heat Mass Transfer*, 11, 805 (1969).
Reischman, M. M., "Laser Anemometer Measurements in Drag-Reducing Channel Flows," Ph.D. thesis, Okla. State Univ., Stillwater (1973).
Shaw, D. A., "Mechanism of Turbulent Mass Transfer to a Pipe Wall at High Schmidt Numbers," Ph.D. thesis, Univ. Ill., Urbana (1976).
Sidahmed, G. H., and R. G. Griskey, "Mass Transfer in Drag Reducing Fluid Systems," *AIChE J.*, 18, 138 (1972).
Smith, K. A., G. H. Keuroghlian, P. S. Virk, and E. W. Merril, "Heat Transfer to Drag-Reducing Solutions," *ibid.*, 15, 294 (1969).
Son, J. S., and T. J. Hanratty, "Limiting Relation for Eddy Diffusivity Close to a Wall," *ibid.*, 13, 689 (1967).
Van Shaw, P., Ph.D. thesis, "A Study of the Fluctuations and the Time Average of the Rates of Mass Transfer to a Pipe Wall," Univ. Ill., Urbana (1963).
Wells, C. S., ed., *Viscous Drag Reduction*, Plenum Press, New York (1969).

Manuscript received September 17, 1976; revision received March 28, and accepted March 30, 1977.

Crystal Size Distribution Dynamics in a Classified Crystallizer:

Part I. Experimental and Theoretical Study of Cycling in a Potassium Chloride Crystallizer

ALAN D. RANDOLPH
JAMES R. BECKMAN
and
ZLATICA I. KRALJEVICH

Department of Chemical Engineering
University of Arizona
Tucson, Arizona 85721

Cycles in particle size and slurry density were experimentally observed in a mixed suspension, potassium chloride crystallizer equipped with a fines dissolver and having nonrepresentative product withdrawal. Cycling behavior was achieved with a product crystal elutriator but was also observed with changes in the orientation of the product removal tube, indicating that instability was induced by product classification. Simulation of the unstable runs with a dynamic model showed crystal size distribution (CSD) limit cycles of similar period using nucleation kinetics and process conditions measured experimentally. The computer simulation showed no tendency towards cycling for the stable runs.

SCOPE

CSD is an important property of an operating crystallizer. Much effort has been spent in reducing CSD transients and eliminating CSD instability in industrial crystallizers in order to make a product within the desired size range at the desired production. Extreme CSD cycling can cause production losses due to off-specification product, overload of dewatering equipment, and exacerbated equipment fouling. Transients of CSD are caused by outside crystallizer upsets (for example, dilution addition, feed rate or composition change, interior fouling, etc.), while unstable CSD's result from the interaction of the system kinetics with the particular crystallizer configuration. The present study demonstrates, both experimentally and theoretically, the phenomenon of low-order cycling wherein CSD instability is caused by the crystallizer configuration (fines destruction and classified product removal) in a stable low-order region of nucleation vs. supersaturation response.

Correspondence should be directed to Dr. Randolph. James R. Beckman is at California State University, Northridge, California.